Phase structure of multiprincipal component AlCoCuFeMnNi alloy prepared by melting casting

MA Ming-Xing1, WANG Zhi-xin1, ZHOU Jia-chen1, LIANG Cun1 and ZHAO Cong2

1School of Materials and Chemical Engineering, Zhongyuan University of Technology, Zhengzhou 450007, China

2School of Chemistry and Environmental Technology, Chongqing University of Arts and Sciences, Chongqing 402160, China

Abstract. AlCoCuFeMnNi high-entropy alloy was fabricated by noon-consumable arc remelter. The phase structure was investigated by x-ray diffraction, and thermodynamic parameters were discussed through caculation in detail. The results show that AlCoCuFeMnNi alloy has two BCC phase structure. The mixing entropy is 13.38J mol-1 K-1, the mixing enthalpy is -2.56kJ mol-1, the atomic radius difference is 0.15, and the Gibbs free energy is -35.73kJ mol-1. The diffraction broad peaks were mainly due to the lattice distortion owing to the atomic radius of each element difference and inhomogeneous diffusion, the increment of residual stress because of cooling rapidly, the small grain size and wide distribution.

Keywords: high entropy; phase structure; microstructure; mechanical alloying

1. INTRODUCTION

High entropy alloys (HEAs) has broken through the design idea of traditional alloy with one or two main elements, and has been formed by various of alloying elements (≥5) with the nearly equal mole ratio (the mole ratio of each component is in the range of 5at%-35at%) [1]. Because of the high entropy effect, the phase number of this system has far below that the predicted phase number by equilibrium phase, which also has a simple solid solution structure (such as BCC, FCC). At the same time, multi-component high entropy alloys have many excellent performance, such as wear resistance and corrosion resistance such as high strength, high hardness, good resistance to high temperature oxidation [2-4], which may open the door of traditional metal materials limit and meet higher demand for materials in the development of industrial technology.

Yeh[1] reported AlxCoCrCuFeNi solid solution alloy had a simple solid solution structure and some excellent properties, and for the first time put forward the concept of high-entropy alloy. And then high-entropy alloy was quickly research focus [5-14], such as alloy microstructure, mechanical properties, corrosion resistance, thermal stability and magnetic properties, and the effect of changes in the proportion of elements and doping and aging on structure and properties. There are relatively few reports on AlCoCuFeMnNi high entropy alloys. In recent years, the mechanical properties of high entropy alloys were studied widely and deeply, and the components of high entropy alloys were focused on Fe, Co, Cr, Ni, Ti, V, Cu and Al. But there were so few of papers reporting to the other components, such as Mn. In this paper, multiprincipal component AlCoCuFeMnNi high entropy alloy was prepared by melting casting method. The phase structure and thermodynamic parameters were discussed in detail. These results will help to provide theoretical guidance of subsequent research for high entropy alloy.

2. EXPERIMENTAL

AlCoCuFeMnNi high-entropy alloy was fabricated by noon-consumable arc remelter. The pure metals of Al, Co, Cu, Fe, Ni and Mn with 200 mesh size and higher purity than 99.5wt% were used as raw materials. The above metal powders having equal molar ratio were mixed by ball milling, compacted, and prepared using WK type non-consumable arc melting furnace under argon environment. The alloy ingot was smelted five times in order to obtain unifrom composition. The cast ingot was cut into 10mm*10mm*5mm block samples by DK7716

electrical discharge machining(EDM). The crystal structure and phase purity of the synthesized samples were identified by x-ray diffraction (XRD) analysis using an Rigaku Ultima IV X-ray diffractometer with Cu Kα radiation operated at 40kV and 30mA. Diffraction data were recorded range from 30 °to 80 °.

Results and discussion

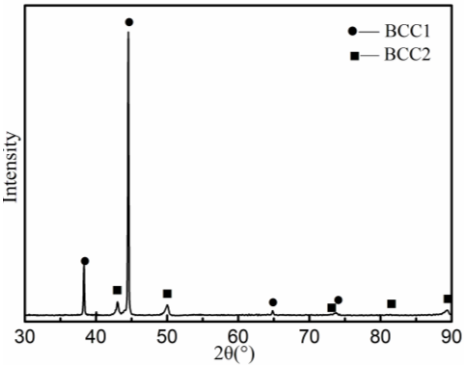

Fig.1 XRD pattern of AlCoCuFeMnNi high-entropy alloy

Fig.1 was XRD pattern of AlCoCuFeMnNi high-entropy alloy. Because AlCoCuFeMnNi alloy was no standard powder diffraction card, and the alloy phase was verified by derivation method. According to the Bragg equation [4,15]:

$$2d\sin\theta = \lambda \quad (1)$$

Where d is the interplanar distance, θ is the diffraction angle, and λ is the wavelength of diffraction target. The relationship between d and interference index was as following:

$$d = a/\sqrt{h^2+k^2+l^2} \quad (2)$$

$$\sin^2\theta = \frac{\lambda^2}{4a^2}\left(h^2+k^2+l^2\right) \quad (3)$$

$$\sin^2\theta_1 : \sin^2\theta_2 : \sin^2\theta_3 : \cdots = (h_1^2+k_1^2+l_1^2) : (h_2^2+k_2^2+l_2^2) : (h_3^2+k_3^2+l_3^2) : \cdots \quad (4)$$

Where a is the lattice constant, h, k and l are the crystal face indexes. Based on lattice extinction rule:

$$(h_1^2+k_1^2+l_1^2) : (h_2^2+k_2^2+l_2^2) : (h_3^2+k_3^2+l_3^2) : \cdots = 3:4:8:11:12:16:\cdots \quad (5)$$

Eq. 5 was belonged to body-centered cubic(BCC) structure. Table 1 was the XRD peak data of AlCoCuFeMnNi high-entropy alloy. These peak data were brought into Eq. 4:

$$\sin^2\theta_1 : \sin^2\theta_2 : \sin^2\theta_3 : \sin^2\theta_4 = 3.00:4.04:8.53:11.02 \quad (6)$$

$$\sin^2\theta_1 : \sin^2\theta_2 : \sin^2\theta_3 : \sin^2\theta_4 : \sin^2\theta_5 = 3.00:4.04:8.70:11.02:12.69 \quad (7)$$

Table 1 XRD peak data of AlCoCuFeMnNi high-entropy alloy

NO.	2θ	θ	Sin2θ	hkl(BCC1)	hkl(BCC2)
1	38.27	19.14	0.011	111	
2	42.98	21.49	0.014		111
3	44.48	22.24	0.015	200	
4	49.95	24.98	0.019		200
5	64.77	32.39	0.032	220	
6	73.53	36.76	0.041		220
7	73.74	36.87	0.041	311	
8	82.92	41.46	0.052		311
9	89.11	44.55	0.060		222

Compared with the lattice extinction rule, the phase structure was composed by two kinds of BCC phases for AlCoCuFeMnNi high-entropy alloy. The diffraction peaks of BCC1 were belonged to (111), (200), (220) and (311) crystal planes. The diffraction peaks of BCC2 were corresponded to (111), (200), (220), (311) and (222) crystal planes. According to the Gibbs phase law [4,16]: F=C-P+1 (which F is the number of degrees of freedom, C is the number of components, and P is the number of phases in thermodynamic equilibrium with each other). Under constant pressure, the maximum phase number in condensed systems can reach C +1. However, it was interesting that the phase structure of AlCoCuFeMnNi alloy was a two-phase solid solution. According to the Gibbs free energy law [16]:

$$\Delta G_{mix} = \Delta H_{mix} - T\Delta S_{mix} \quad (8)$$

Where ΔHmix is the mixing enthalpy, T is the thermodynamic temperature, and ΔSmix is the mixed entropy. From the Eq. 8, the mixing enthalpy and the mixed entropy were two competition factors for the change of the system free energy. There was beneficial to the reduce of system free energy, alloy ordering and segregation trend with the increment of the mixed entropy especially at high temperature, which made the disordered solid solution formed easily compared with the intermetallic compounds during solidification. Based on the Boltzmanna hypothesis of the relationship between entropy and system confusion, the alloy mixed entropy ΔSmix can be expressed as [16]:

$$\Delta S_{\text{mix}} = -R\sum_{i=1}^{n} c_i \ln c_i \quad (9)$$

$$\Delta S_{\text{mix}} = R\ln n \quad (10)$$

Where ci is the mole percent of the i-th component in the alloy system ($\sum_{i=1}^{n} c_i = 1$), and R is the gas constant. When *c1=c2=...=ci*, the mixed entropy can reach the maximum value. The mixing enthalpy ΔHmix can be expressed as [4,16]:

$$\Delta H_{mix} = \sum_{i=1, i\neq j}^{n} \Omega_{ij} c_i c_j \quad (11)$$

$$\Omega_{ij} = 4\Delta H_{AB}^{mix} \quad (12)$$

Where Ωij is the interaction parameter of component between the i-th and the j-th elements, ΔH_{AB}^{mix} is the enthalpy of mixing for the binary equal atomic A-B alloy calculated by the Miedema model[17]. Table2 was the mixed enthalpy between the various elements[17]. According to the Hume-Ruthery rule, the atomic radius difference δ can be expressed as:

$$\delta = \sqrt{\sum_{i=1}^{n} c_i (1 - \frac{r_i}{\bar{r}})^2} \quad (13)$$

$$\bar{r} = \sum_{i=1}^{n} c_i r_i \quad (14)$$

Where ri is the atomic radius of i component, $\bar{r}$ is the average atomic radius of the alloy components. Table3 was the element characteristic parameters of AlCoCuFeMnNi alloy. From Eq. 8-14, the mixing entropy is 13.38J mol-1 K-1, the mixing enthalpy is -2.56kJ mol-1, the atomic radius difference is 0.15, and the Gibbs free energy is -35.73kJ mol-1 for AlCoCuFeMnNi high-entropy alloy.

Table2 Mixed enthalpy between the various elements[17] (kJ/mol)

	Al	Co	Cu	Fe	Mn	Ni
Al	−	-19	-1	-11	-19	-22
Co	-19	−	6	-1	-5	0
Cu	-1	6	−	13	4	4
Fe	-11	−1	13	−	0	-2
Mn	−19	-5	4	0	−	-8
Ni	-22	0	4	-2	-8	−

Table3 Element characteristic parameters of AlCoCrCuFe alloy

Element	Melting point (℃)	Electronegativity	Atomic radius(nm)	Lattice structure
Al	660	1.61	0.143	FCC
Co	1495	1.88	0.125	HCP/BCC
Cu	1083	1.90	0.128	FCC
Fe	1535	1.83	0.127	BCC/FCC
Mn	1244	1.55	0.126	BCC
Ni	1453	1.92	0.125	FCC

In addition, the diffraction peaks of AlCoCuFeMnNi high-entropy alloy were broad peaks. This was mainly due to: (1) the lattice distortion owing to the atomic radius of each element difference; (2) the lattice distortion as a result of inhomogeneous diffusion. The peak intensity decreased and the peak width increased because the degree of crystallinity was reduced with increasing of lattice distortion; (3) the increment of residual stress because of cooling rapidly [18,19]; (4) the small grain size and wide distribution.

CONCLUSION

The phase structure of AlCoCuFeMnNi high-entropy alloy was composed by two kinds of BCC phases. The diffraction peaks of BCC1 were belonged to (111), (200), (220) and (311) crystal planes. The diffraction peaks of BCC2 were corresponded to (111), (200), (220), (311) and (222) crystal planes. the mixing entropy is 13.38J mol-1 K-1, the mixing enthalpy is -2.56kJ mol-1, the atomic radius difference is 0.15, and the Gibbs free energy is -35.73kJ mol-1 for AlCoCuFeMnNi high-entropy alloy. The diffraction broad peaks were mainly due to the lattice distortion owing to the atomic radius of each element difference and inhomogeneous diffusion, the increment of residual stress because of cooling rapidly, the small grain size and wide distribution.

REFERENCES

[1] J.W. Yeh, S.K. Chen, S.J. Lin, et al, Nanostructured high-entropy alloys with multiple principal elements: novel alloy design concepts and outcomes. Adv. Eng. Mater. 6(2004): 299-303.

[2] B. Gludovatz, A. Hohenwarter, D. Catoor, et al, A fracture-resistant high-entropy alloy for cryogenic applications, Science, 345(2014):1153-1158.
[3] C.W. Lin, M.H. Tsai, C.W. Tsai, et al, Microstructure and aging behaviour of AlCrFeNiTi high entropy alloy, Mater. Sci. Technol. 31(2015):1165-1170
[4] Y. Zhang, X. Yang, P.K. Liaw, Alloy design and properties optimization of high-entropy alloys, JOM, 64 (2012) :830-838
[5] G.H. Meng, X. Lin, H. Xie, et al, The effect of Cu rejection in laser forming of AlCoCrCuFeNi/Mg composite coating, Mater. Des. 108(2016): 157-167
[6] G. Li, D.H. Xiao, P.F. Yu, et al, Equation of state of an AlCoCrCuFeNi high-entropy alloy, JOM, 67(2015):2310-2313
[7] Y. Deng, C.C. Tasan, K.G. Pradeep, et al, Design of a twinning-induced plasticity high entropy alloy, Acta Mater. 94(2015):124-133
[8] M.J. Yao, K.G. Pradeep, C.C. Tasan, et al, A novel, single phase, non-equiatomic FeMnNiCoCr high-entropy alloy with exceptional phase stability and tensile ductility, Scripta Mater. s72-73 (2014) :5-8
[9] L. Xie, P. Brault, A.L. Thomann, et al, AlCoCrCuFeNi high entropy alloy cluster growth and annealing on silicon: A classical molecular dynamics simulation study. Appl. Surf. Sci. 285 (2013) :810-816
[10] R.S. Ganji, P.S. Karthik, K.B.S. Rao, et al, Strengthening mechanisms in equiatomic ultrafine grained AlCoCrCuFeNi high-entropy alloy studied by micro- and nanoindentation methods, Acta Mater. 125(2017):58-68
[11] Y.J. Zhou, Y. Zhang, Y.L. Wang, et al, Solid solution alloys of AlCoCrFeNiTix with excellent room-temperature mechanical properties, Appl. Phys. Lett. 90 (2007):181904
[12] T.M. Yue, H. Xie, X. Lin, et al. Solidification behaviour in laser cladding of AlCoCrCuFeNi high-entropy alloy on magnesium substrates, J. Alloys Compd. 587(2014):588-593
[13] J.M. Zhu, H.F. Zhang, H.M. Fu, et al. Microstructures and compressive properties of multicomponent AlCoCrCuFeNiMox alloys, J. Alloys Compd. 497(2010):52-56
[14] L.H. Wen, H.C. Kou, J.S. Li, et al. Effect of aging temperature on microstructure and properties of AlCoCrCuFeNi high-entropy alloy, Intermetallics, 17(2009):266-269
[15] M.X. Ma, D.C. Zhu, M.J. Tu. The effect of Eu2+ doping concentration on luminescence properties of BaAl2Si2O8:Eu2+ blue phosphor, Acta Phys. Sin.-Ch. Ed. 58 (2009) :5826-5830
[16] Y. Zhang, Y. Zhou, J. Lin, et al, Solid-solution phase formation rules for multi-component alloys, Adv. Eng. Mater. 10(2010) :534-538
[17] A. Takeuchi, A. Inoue, Classification of bulk metallic glasses by atomic size difference, heat of mixing and period of constituent elements and its application to characterization of the main alloying element, Mater. Trans. 46(2005): 2817-2829
[18] Q.Y. Zhai, C. Jia, Z.X. Kang, et al. Microstructure and capacitor discharge\par welding characteristics of quenched Cu25Al10Ni25Fe20Co20 high-entropy alloy foils, Acta Metall. Sin. 47 (2011) :1378-1381
[19] M.X. Ma, D.C. Zhu, C. Zhao, et al. Effect of Sr2+-doping on structure and luminescence properties of BaAl2Si2O8:Eu2+ phosphors, Opt. Commu. 285(2012):665-668.